

Electromediated formation of DNA complexes with cell membranes and its consequences for gene delivery

Jean-Michel Escoffre¹

Institut de Pharmacologie et de Biologie Structurale, CNRS, Université de Toulouse, UPS, Toulouse, France

Thomas Portet¹

Institut de Pharmacologie et de Biologie Structurale and Laboratoire de Physique Théorique, CNRS, Université de Toulouse, UPS, Toulouse, France

Cyril Favard¹

Institut Fresnel, CNRS, Universités Aix-Marseille, Marseille, France

Justin Teissié

Institut de Pharmacologie et de Biologie Structurale, CNRS, Université de Toulouse, UPS, Toulouse, France

David S. Dean

Laboratoire de Physique Théorique, CNRS, Université de Toulouse, UPS, Toulouse, France

Marie-Pierre Rols*

Institut de Pharmacologie et de Biologie Structurale, CNRS, Université de Toulouse, UPS, Toulouse, France

Abstract

Electroporation is a physical method to induce the uptake of therapeutic drugs and DNA, by eukaryotic cells and tissues. The phenomena behind electro-mediated membrane permeabilization to plasmid DNA have been shown to be significantly more complex than those for small molecules. Small molecules cross the permeabilized membrane by diffusion whereas plasmid DNA first interacts with the electroporeabilized part of the cell surface, forming localized aggregates. The dynamics of this process is still poorly understood because direct observations have been limited to scales of

*Corresponding author

Email address: Marie-Pierre.Rols@ipbs.fr, Fax : +33 (0) 561 175 994, Tel : +33 (0) 561 175 811 (Marie-Pierre Rols)

¹The first three authors made an equal contribution to this paper

the order of seconds. Here, cells are electroporated in the presence of plasmid DNA and monitored with a temporal resolution of 2 ms. This allows us to show that during the first pulse application, plasmid complexes, or aggregates, start to form at distinct sites on the cell membrane. FRAP measurements show that the positions of these sites are remarkably immobile during the application of further pulses. A theoretical model is proposed to explain the appearance of distinct interaction sites, the quantitative increase in DNA and also their immobility leading to a tentative explanation for the success of electro-mediated gene delivery.

Keywords: Electroporation; DNA transfer; modeling; fluorescence microscopy

1. Introduction

Electroporation is the phenomena by which the application of an electric field across a biological membrane renders it permeable to the passage of small and even macro molecules such as DNA [1, 2]. It is exploited in the clinical context where the permeabilization of cells to a therapeutic agent is required, for example in gene therapy and chemotherapy [3, 4, 5]. Despite the use of electroporation in medical science, many questions remain open as to the underlying biophysicochemical phenomena which underpin its success. This is especially the case for the permeabilization of membranes to DNA where a number of interesting biological, chemical and physical factors remain to be understood. Given the size of the DNA, if the permeabilization is due to pores – or conducting defects–, as suggested by the standard theory of electroporation [6, 7], the pores must be relatively large due to (i) the relatively large size of the DNA and (ii) the large charge of DNA as dielectric exclusion must be overcome [8]. The cell membrane has a much more complex organization than a model lipid bilayer. One expects that the location of regions permeabilized to DNA will be determined not only by the local electric field but also by the local membrane composition. In cell membranes, the regions most susceptible to permeabilization may be those containing certain types of transmembrane proteins or at the boundary between differing types of lipid domains [9]. Another key, physicochemical factor is how the field not only modifies the permeability of the membrane, but also how it influences

the movement of the DNA by electrophoresis. Large polyelectrolytes are strongly advected by the electric field [10]. Experimental studies [11] have demonstrated that the physicochemical phenomena involved in electro-mediated membrane permeabilization to plasmid DNA are indeed significantly more complex than those for small molecules. Small molecules cross the permeabilized membrane directly mainly by post-pulse diffusion, whereas plasmid DNA first interacts with the electropermeabilized part of the cell surface resulting in the formation of localized aggregates. However the dynamics of this initial interaction is only partially understood because the direct observations of [11] were limited to time scales exceeding several seconds. In this paper, we have analyzed the interaction between the cell membrane and strongly charged macromolecules (4.7 kbp plasmid DNA) upon the application of a permeabilizing electric field, at a temporal resolution of 2 ms. This enables us to address the following unresolved, and key, questions (i) What are the phenomena leading to formation of the sites where the DNA aggregates? (ii) What is the underlying dynamics behind their formation? (iii) To what extent are the sites localized in space, and over what time scales? and (iv) What is the biochemical mechanism behind this localization? We put forward a model for the transport of charged molecules in the presence of the electric field which provides an interpretation for most of our experimental findings on DNA and whose validity is also tested via additional experiments using the, much smaller, charged molecule Propidium Iodide.

2. Materials and methods

2.1. Cells

Chinese hamster ovary (CHO) cells were used. The WTT clone was selected for its ability to grow in suspension or plated on Petri dishes or on a microscope glass coverslip. Cells were grown as previously described [12]. For microscopy experiments, 10^5 cells were put on a Lab-tek chamber 12 hours before electric pulse treatment with 1 ml of culture medium.

2.2. DNA staining

A 4.7 kbp plasmid (pEGFP-C1, Clontech, Palo Alto, CA) carrying the green fluorescent protein gene controlled by the CMV promoter was stained stoichiometrically with the DNA intercalating dye TOTO-1 (or alternatively POPO-3) (Molecular Probes, Eugene, OR) [13]. The plasmid was stained with 2.3×10^{-4} M dye at a DNA concentration of $1 \mu\text{g}/\mu\text{l}$ for 60 minutes on ice. This concentration yields an average base pair to dye ratio of 5. Even if the labeling is not covalent, the equilibrium is dramatically in favor of the linked form. Plasmids were prepared from *E. Coli* transfected bacteria by using Maxiprep DNA purification system (Qiagen, Chatsworth, CA).

2.3. Electroporabilization apparatus.

Electropulsation was carried out with a CNRS cell electropulsator (Jouan, St Herblain, France) which delivers square-wave electric pulses. An oscilloscope (Enertec, St. Etienne, France) was used to monitor the pulse shape. The electropulsation chamber was built using two stainless-steel parallel rods (diameter 0.5 mm, length 10 mm, inter-electrode distance 5 mm) placed on a Lab-tek chamber. The electrodes were connected to the voltage generator. A uniform electric field was generated. The chamber was placed on the stage of an inverted digitized videomicroscope (Leica DMIRB, Wetzlar, Germany) or a confocal microscope (Zeiss, LSM 5 life, Germany).

2.4. Electroporabilization

Permeabilization of cells was performed by application of millisecond electric pulses required to transfer genes and to load macromolecules into cells. Cell viability was preserved when using millisecond pulse duration by decreasing the electric field intensity [14, 15]. Penetration of PI ($100 \mu\text{M}$ in a low ionic strength pulsing buffer: 10 mM phosphate, 1 mM MgCl_2 , 250 mM sucrose, pH 7.4) was used to monitor permeabilization. 10 pulses of 20 ms duration and 0.5 kV/cm amplitude were applied at a frequency of 1 Hz at room temperature. For plated cells, the culture medium was removed and replaced by the same buffer described above.

2.5. Microscopy

Cells were observed with a Leica 100 \times , 1.3 numerical aperture oil immersion objective. Images (and optical sections) were recorded with the CELLscan System from Scanalytics (Billerica, MA) fitted with a cooled CCD camera (Princeton Instrument, Trenton, NJ). This digitizing set up allowed a quantitative localized analysis of the fluorescence emission as described previously [11]. This was done along the cell membrane. Images were taken at a 1 Hz frequency. For fast kinetics studies, a Zeiss LSM 5 Live confocal microscope was used. All measurements were performed at room temperature. Image sequences were acquired at a frequency of 500 fps.

2.6. FRAP experiments

FRAP experiments were performed on a Zeiss LSM 510 confocal microscope. The 488 nm line of the Ar⁺ laser was used for excitation of TOTO-1. We used a sequential mode of acquisition with a 63 \times , 1.4 numerical aperture water immersion lens. After 50 pre-bleach scans, a region of interest (ROI) with a radius $w = 1\mu\text{m}$ was bleached, and fluorescence recovery was sampled on 150 scans, *i.e.* 40 s [16].

2.7. Actin cytoskeleton destabilization

To examine the role of actin in the phenomenon of DNA membrane interaction, cells were incubated at 37 $^{\circ}$ C for 1 hour with 1 μM Latrunculin A (Sigma) in culture medium. This protocol is known to efficiently disrupt the actin cytoskeleton [17].

3. Experimental results

3.1. Electropulsation experiments

To study membrane permeabilization by electric fields, and the associated processes of molecular uptake, we used PI and TOTO-1 labelled plasmid DNA. Membrane permeabilization was induced by applying 20 ms electric pulses of intensity 0.5 kV/cm. This protocol is known to induce both membrane permeabilization and DNA transfer, accompanied by an associated gene expression [11]. Membrane permeabilization was observed at the single cell level at a rate of 500 frames per second. This image acquisition frequency made it possible to monitor the entire process of molecular uptake, both

during and after pulse application, with a good spatial resolution using confocal microscopy. Particular attention was paid to the molecular uptake occurring after a single permeabilizing pulse and a series of 10 pulses.

3.2. Electropulsation experiments with PI

As shown in Figs. 1A and 1C, and in agreement with previous studies [11], membrane permeabilization, as detected by the uptake of PI, was observed at sites of the cell membrane facing the two electrodes. The influx into the cells of PI, deduced from the associated fluorescence intensity, suggests free transport across the permeabilized regions of the membrane into the cytoplasm (no trapping in the region near the membrane is observed). The uptake of PI into cells started at the moment the pulse was applied and the concentration of PI in the cell increased for up to a minute (Fig. 1E), showing that the permeabilized membrane state, due to defect regions such as metastable pores, persists for some time after the field is cut. Indeed, the majority of molecules which were taken up entered the cell after the pulses. Analyzing the molecular uptake image by image led to the observation that PI uptake was both asymmetric and delayed: it was higher at the anode facing side of the cell and its entrance at the cathode facing side occurred after a 4-5 second delay. This asymmetry can be explained by the fact that PI has a charge $+2e$ in solution and thus the electrophoretic force drives it toward the cathode. The post-pulse diffusion of PI into the cytoplasm of the permeabilized cell can be seen in Movie 1 (published in supporting information).

3.3. Electropulsation experiments with DNA

Electro-induced uptake by cells in presence of plasmid DNA showed results that differed considerably from those for cells pulsed in presence of PI. DNA was only observed to interact with the membrane for electric fields greater than a critical value (0.25 kV/cm) which induces their permeabilization, i.e. leading to PI uptake. In the low field regime DNA simply flowed around the cells towards the anode. For permeabilizing fields, plasmid DNA was not observed to enter the cell during pulse application or during the minute that followed. However, DNA was seen to accumulate at distinct sites on the cathode facing side of the permeabilized cell membrane (Fig. 1D). At these

sites the DNA appeared to form aggregates, which became visible as soon as the electric pulse was triggered (Fig. 2A, 2B). Intriguingly, the number and apparent size of these sites did not increase with the number of pulses applied. During the application of a single pulse, the fluorescence of the sites increased linearly in time showing that the quantity of DNA at each site increased linearly (Fig. 1F), but no such fluorescence increase was observed in the absence of the electric field. Therefore the accumulation of DNA at the interaction sites must be principally due to electrophoresis.

The presence of stable sites, where membrane plasmid DNA interaction occurred, was observed across the entire cell population (Fig. 1D) (see Movie 2 in supporting information). The average distance between a site and its nearest neighbor was found to be about 1 μm . The diameter of the individual sites was found to be in the range of 300-600 nm (lower range limit due to optical diffraction). As shown in Fig. 2C, the total amount of DNA in the membrane region also increased linearly with the number of electric pulses. The final average amount of DNA localized in the membrane region correlated with the amount of DNA reaching the nucleus, as estimated by the rate of GFP expression, between 2 and 24 hours after pulse application (see supplementary information).

As shown in Figs. 1E and 1F, part of the DNA interacting with the membrane was observed to be desorbed after the pulses but a large proportion stayed fixed, this could be due to an interaction between the membrane and DNA but also because the DNA forced into the pore electrophoretically is virtually immobile in the cell in the absence of the electric field. This last observation shows that the observed DNA membrane interaction could be, at least partially, due to (i) electrophoretic accumulation along with (ii) reduced mobility of the DNA in the pore region within the cell.

We also studied the mobility of the DNA complexes at the interaction sites. In order to measure the in-membrane or lateral diffusion constant of the complexes, we carried out Fluorescence Recovery After Photobleaching (FRAP) experiments. The FRAP results showed that no exchange between DNA aggregates or with the bulk DNA took place and that the DNA was, on experimental time scales, totally immobile, its lateral diffusion coefficient being less than $10^{-16}\text{m}^2\text{s}^{-1}$. This could be explained by the reduced mobility of individual DNA molecules within the cell or because DNA

forms micro sized aggregates which are immobile due to their large size. It is unlikely that this immobility is due to an intrinsic immobility of pores, as the measured diffusion constant is orders of magnitude smaller than the typical values reported in the literature for transmembrane objects, such as proteins.

One could argue that actin polymerization around inserted DNA may be responsible for its immobilization at the membrane level as well as in its subsequent traffic inside the cytoplasm. However, actin cytoskeleton perturbation with Latrunculin A did not seem to modify the features of DNA spot creation, their stability or immobility (see supplementary information). This implies that, despite the fact that actin causes a drastic decrease in the mobility of individual large DNA molecules inside cells, the initial formation of DNA spots and their immobility is not caused by the actin network.

4. Theoretical analysis

4.1. Theoretical model

In order to better understand the features of the electro-mediated DNA uptake, we developed a theoretical model that we used to carry out numerical simulations. We assumed that the cell membrane was an infinitesimally thin non-conducting surface. This approximation is valid where the membrane thickness is small compared to all other length scales and the conductivities of the cell interior σ_i and exterior electropulsation solution σ_e are much greater than the conductivity σ_m of the cell membrane. An electric field of magnitude $|\mathbf{E}_0| = E_0$ is applied in the z direction, perpendicular to the electrodes, and the local electric potential ϕ is given, in the steady state regime, by the solution to Laplace's equation [18]

$$\nabla \cdot \sigma \nabla \phi = 0, \quad (1)$$

with the boundary conditions $\phi = -E_0 z$ as $|z| \rightarrow \infty$. In what follows we will assume that the DNA is advected by the field given by the solution of Laplace's equation (1) and will neglect additional fields that would be caused by local accumulation of charge due to the DNA. This is because the applied fields are relatively large and because we expect the DNA to be strongly screened. Once the electric field has been computed the

DNA is advected by the field but also diffuses. The local concentration of DNA $c(\mathbf{x}, t)$ obeys the electrodiffusion equation

$$\frac{\partial c}{\partial t} = -\nabla \cdot \mathbf{j} \quad (2)$$

where \mathbf{j} is the thermodynamic current $\mathbf{j} = -D\nabla c + \mu c \mathbf{E}$, with D the local diffusion constant of the DNA, which depends on its environment, and is denoted by D_e outside the cell, D_m in the membrane and D_i in the cell interior. The term μ is the electrophoretic mobility and is defined via the velocity \mathbf{v} of the molecule in a (locally) uniform field $\mathbf{E} = -\nabla \phi$ as

$$\mathbf{v} = \mu \mathbf{E}. \quad (3)$$

As for the diffusion constant, the value of μ will also depend on the local environment as it depends on electrolyte concentration and viscosity. As the electrode system is in contact with a bath of the transported molecule we impose the boundary conditions $\nabla c = 0$ as $c \rightarrow \infty$ on equation (2) (note that this is compatible with the Ohmic behavior $\mathbf{j} = \mu c \mathbf{E}$ far from the cell). We assume that D_m and $\mu_m = 0$, which means that DNA cannot move into intact regions of membrane.

4.2. Modeling pores

We will assume that when the field is applied, the membrane becomes permeabilized and micro sized pores are formed. For the ease of computation we will investigate what happens when a circular pore is formed at each face of the cell facing the electrodes, that facing the anode in the angular region $\theta \in [0, \theta_p]$ and that facing the cathode in the region $\theta \in [\pi - \theta_p, \pi]$. In this region we assume that the conductivity is σ_i and that the diffusion constant is D_i , effectively we have taken away the membrane from these regions and replace it by the cellular interior. We numerically compute the evolution of the concentration of marker molecules as a function of time using the experimental applied field protocols (we assume that the membrane charging process is much quicker than any of the diffusion processes and thus change the electric field instantaneously).

Estimation of theoretical parameters. We were able to follow the fluorescence of the DNA in the buffer solution in a uniform electric field and thus measure its velocity. Using equation (3). we estimated the electrophoretic mobility in solution to be $\mu_e =$

$10^{-8} m^2 V^{-1} s^{-1}$. This agrees with more precise measurements reported in the literature [19]. The diffusion constant of DNA in aqueous solution is estimated from the literature to be $D_e = 10^{-12} m^2 s^{-1}$ [20].

The charge of the PI is taken to be $q = +2e$ and its diffusion constant in aqueous solution is estimated to be $D_e = 10^{-10} m^2 s^{-1}$ (by estimating its effective radius and using the Stokes formula for the diffusion constant of a solid sphere). The electrophoretic mobility for PI is estimated via the Stokes Einstein relation $\mu = \frac{qD}{k_B T}$ where k_B is Boltzmann's constant and T is the temperature.

In the cell interior we estimate that for PI the effective diffusion constants and electrophoretic mobilities are smaller than their external values by a factor of 10 but for the larger DNA molecules they are smaller by a factor of 1 000 (in fact this factor is a lower bound) due largely to the interaction between the DNA and the actin network of the cell interior [20, 21]. Finally we took the radius of the spherical vesicle to be $R = 8 \mu m$ as estimated from the average cell size.

4.3. Theoretical results and comparison with experiments

We assume that the marker fluorescence is proportional to the concentration $c(\mathbf{x}, t)$. For the comparison with the experiments we took a pore angle $\theta_p = 3.6^\circ$ as estimated by the size of the DNA/membrane interaction sites we observed. We computed the average fluorescence intensity inside the cell using $I_{cell} \propto c_{cell}$. In Figs. 1G and 1H we show the predicted behavior for PI fluorescence for one pulse with applied field $0.5 kV cm^{-1}$ applied for $20 ms$ and see that it compares very well with that measured experimentally (Fig. 1 E). Similarly we see in the same figures the comparison between theory and experiment is also good for DNA (with the same pulse protocol), with the exception that the slight decrease in DNA fluorescence after the pulse has been applied is less pronounced in the theoretical curve of Fig. 1F. However some of the experimentally observed decrease may be due to photo bleaching of the fluorescent marker. Note that although we have only simulated one pore, if we assume that the pores behave independently (as conduction channels in parallel) the overall form of the increase in fluorescence for several pores should be approximately of the same form, up to an overall change in the fluorescence levels, as that for single pore.

In the case of PI, our model also reproduced the other qualitative behavior seen in the experiments. Numerical calculations showed that the PI enters through the anode facing side of the vesicle during the pulse application and that its entry into the cathode facing side is delayed, as expected from the physical arguments given in the Results section.

For DNA, computations showed that just after the field application there is virtually no uptake of DNA at the anode facing side of the cell, but that at the cathode facing side there is an accumulation of DNA near the surface of the cell in the region where the pore is. In our model the DNA accumulation, apparently, at the surface of the cell, is due to the strong (as compared to the case of PI) electrophoretic force which pushes the DNA into the hole opposite the cathode and then the much reduced mobility of the DNA in this region. For DNA most of the contribution to the total cell fluorescence comes from the region close to the membrane surface, thus justifying our comparison of Figs. 1E, 1F with Figs. 1G, 1H.

4.4. Constant number of interaction sites

The experimental results show that after the first interaction sites become visible, no further sites appear during subsequent pulsation. An explanation for this is that the pores formed are conducting and thus the electric field across the membrane is lowered in the non-conducting regions of the membrane. A simple criterion for determining whether a membrane can be locally permeabilized is if the stress caused by the electric field causes the local surface tension to exceed the lysis tension of the membrane. In a simple electric model for the membrane this turns out to be equivalent to the local transmembrane voltage $\Delta\phi$ exceeding a critical value $\Delta\phi_c$, which has values typically between 250 – 1000 mV [22, 23]. To see how the presence of a pore reduces the transmembrane potential elsewhere we consider the simplified case of an infinitesimally thin, non-conducting, infinite flat membrane with a conducting pore of radius a . The potential drop across the membrane at a distance r from the center of the pore is [24] $\Delta\phi(r) = \frac{2\Delta\phi_o}{\pi} \arctan(\frac{\sqrt{r^2 - a^2}}{a})$, where $\Delta\phi_o$ is the potential drop far from the pore (or in the absence of the pore) and we assume that $\Delta\phi_o > \Delta\phi_c$. If pores can only be formed in regions where $\Delta\phi > \Delta\phi_c$ one sees that this critical potential drop cannot be exceeded

within in a radius $r_c = \frac{a}{\cos(\frac{\pi\Delta\phi_c}{2\Delta\phi_0})}$ from the center of the pore. Although a very approximate estimate, this shows that we should expect pores to be separated from each other by a distance of the order of the pore size. This is indeed the case as can be seen in Fig. 2B, where the fluorescence peaks widths are of the same order as the inter-peak distance.

5. Discussion

Despite the complexity of the system studied here, a number of our experimental observations can be explained qualitatively and to an extent quantitatively on a largely physical basis. According to the standard theory of electroporation, the effect of the electric field is to render the cell membrane permeable to external molecules via the formation of micro sized pores. Another effect of the electric field on the DNA is an electrophoretic one, DNA is pushed toward the cathode facing side of the cell and, as our numerical calculations have shown, if a sufficiently large pore is present the DNA can be forced through it. However once the DNA is inside the cell it stays, on experimental time scales, very close to the surface either due to the reduced electrophoretic mobility and diffusion constant of individual DNA molecules caused by the actin cytoskeleton or because it forms aggregates which are immobile due to their large size. The number of DNA interaction sites remains constant even on increasing the number of pulses, we have argued that this is because these sites are conducting, the electric field elsewhere in the cell membrane is reduced by the presence of these conducting sites and thus does not exceed the threshold value necessary to form additional permeabilized regions and thus interaction sites.

Results on cells where the actin cytoskeleton is disrupted also show spot formation and so we conclude that the principal mechanism for spot formation is the formation of aggregates where the DNA molecules are bound together and thus diffuse as a macroscopic object with a very small diffusion constant. A possible mechanism for this aggregation is the presence of multivalent cations induced by the high concentration of DNA in the pore region [25].

To conclude we have been able to provide a detailed explanation of why gene ther-

apy using electropulsation is successful. The process of plasmid transfer through the cellular cytoplasm to the nuclear envelope is a complex process [26, 27]. In principle micro sized aggregates of DNA or vesicles filled with DNA could be too large to pass through the pores formed by electroporation. However individual DNA molecules, while they can pass through electropores, have a limited mobility within the cell and may well be totally degraded before reaching the nucleus. It is possible and worth investigating the possibility that the actin cytoskeleton reacts to the presence of DNA aggregates and plays an important role in the subsequent intracellular transport. It seems reasonable that only aggregates beyond a certain size (a few hundred nano-meters) can induce a biological cellular response and can be transported by the cell. In addition, the fact that the DNA is in aggregate form means that the DNA in the center of the aggregate is relatively protected from degradation. Therefore, for gene therapy purposes, it is optimal for DNA to enter the cell as single molecules, but the subsequent transport toward the nucleus is, for biological (possibly by inducing a response of the actin cytoskeleton) and physical (diminishing enzymatic degradation) reasons, optimized if the DNA is in a micro-sized aggregate form.

We thus see that a rather beautiful and subtle, and to an extent fortuitous, combination of biological, chemical and physical factors may underpin the success of gene therapy via electropulsation. As our understanding of these underlying phenomena advances we should be able to refine and optimize the protocols used in electro-mediated gene therapies.

6. Acknowledgements

Our group belongs to the CNRS consortium Celltiss. This work has benefitted from the financial support of the Association Française contre les Myopathies, the Region Midi-Pyrenees and the Institut Universitaire de France. We wish to thank Gabor Forgacs for useful discussions on this work.

References

- [1] Neumann, E., A.E. Sowers, and C.A. Jordan, 1989. *Electroporation and electrofusion in cell biology* (Plenum, New York).
- [2] Weaver J.C., 1995. Electroporation theory. Concepts and mechanisms. *Methods Mol. Biol.* 55:3–28.
- [3] Belehradek, M., C. Domenge, B. Luboinski, S. Orlowski, J. Belehradek and L. Mir, 1993. Electrochemotherapy, a new antitumor treatment. First clinical phase I-II trial. *Cancer* 72:3694–3700.
- [4] Daud, A.I., R.C. DeConti, S. Andrews, P. Urbas, A.I. Riker, V.K. Sondack, P.N. Munster, D.M. Sullivan, K.E. Ugen, I.J. Messina and R. Heller, 2008. Phase I trial of interleukin-12 plasmid electroporation in patients with metastatic melanoma. *J. Clin. Oncol.* 26:5896–5903.
- [5] Rols M.P., 2006. Electropermeabilization, a physical method for the delivery of therapeutic molecules into cells. *Biochim. Biophys. Acta* 1758:423–428.
- [6] Pastushenko, V.F., Y.A. Chizmadzhev and V.B. Arekelyan, 1979. Electric breakdown of bilayer membranes II. Calculation of the membrane lifetime in the steady-state diffusion approximation. *Bioelectrochem. Bioenerg.* 6:53–62.
- [7] Powell, K.T. and J.C. Weaver, 1986. Transient aqueous pores in bilayer membranes: a statistical theory. *Bioelectrochem. Bioenerg.* 15 : 211–227.
- [8] V.A. Parsegian, 1969. Energy of an ion crossing of a low dielectric membrane: Solutions to four relevant electrostatic problems. *Nature* 221:844–846.
- [9] Antonov, V.F., W. Petrov, A.A. Molnar, D.A. Predvoditelev and A.S. Ivanov, 1980. Appearance of single-ion channels in unmodified lipid bilayer-membranes at the phase transition temperature. *Nature* 283:585–586.
- [10] Gabriel, B. and J. Teissié, 1999. Time courses of mammalian cell electropermeabilization observed by millisecond imaging of membrane property changes during the pulse. *Biophys. J.* 76:2158–2165.

- [11] Golzio, M., J. Teissié and M.P. Rols, 2002. Direct visualization at the single-cell level of electrically mediated gene delivery. *Proc. Natl. Acad. Sci. U S A* 99:1292–1297.
- [12] Rols, M.P., D. Coulet and J. Teissié, 1992. Highly efficient transfection of mammalian cells by electric field pulses. Application to large volumes of cell culture by using a flow system. *Eur. J. Biochem.* 206:115–121.
- [13] Rye, H.S., S. Yue, D.E. Wemmer, M.A. Quesada, R.P. Haugland, R.A. Mathies and A.N. Glazer, 1992. Stable fluorescent complexes of double-stranded DNA with bis-intercalating asymmetric cyanine dyes: properties and applications. *Nucleic Acids Res.* 20:2803–2812.
- [14] Wolf, H., M.P. Rols, E. Boldt, E. Neumann and J. Teissié, 1994. Control by pulse parameters of electric field-mediated gene transfer in mammalian cells. *Biophys. J.* 66:524–531.
- [15] Golzio, M., M.P. Mora, C. Raynaud, C. Delteil, J. Teissié and M.P. Rols, 1998. Control by osmotic pressure of voltage-induced permeabilization and gene transfer in mammalian cells. *Biophys. J.* 74:3015–3022.
- [16] Causeret, M., N. Taulet, F. Comunale, C. Favard and C. Gauthier-Rouviere, 2005. N-cadherin association with lipid rafts regulates its dynamic assembly at cell-cell junctions in C₂C₁₂ myoblasts. *Mol. Biol. Cell.* 16:2168–2180.
- [17] Sun, M., N. Northup, F. Marga, T. Huber, F.J. Byfield, I. Levitan and G. Forgacs, 2007. The effect of cellular cholesterol on membrane-cytoskeleton adhesion. *J. Cell Sci.* 120:2223–2231.
- [18] Landau, L.D. and E.M. Lifshitz, 1975. *Electrodynamics of Continuous Media* (Pergamon Press, Oxford).
- [19] Stellwagen, N.C., C. Gelfi and P.G. Righetti, 1997. The free solution mobility of DNA. *Biopolymers* 42:687–703.

- [20] Lukacs, G.L., P. Haggie, O. Seksek, D. Lechardeur, N. Freedman and A.S. Verkman, 2000. Size-dependent DNA mobility in cytoplasm and nucleus. *J. Biol. Chem.* 275:1625–1629.
- [21] Dauty, E. and A.S. Verkman, 2005. Actin cytoskeleton as the principal determinant of size-dependent DNA mobility in cytoplasm. *J. Biol. Chem.* 280:7823–7828.
- [22] Teissié, J. and M.P. Rols, 1993. An experimental evaluation of the critical potential difference inducing cell membrane electroporation. *Biophys. J.* 65:409–413.
- [23] Portet, T., F. Camps Febrer, J.M. Escoffre, C. Favard, M.P. Rols and D.S. Dean, 2009. Visualization of membrane loss during the shrinkage of giant vesicles under electroporation. *Biophys. J.* 96:4109-4121.
- [24] Winterhalter, M. and W. Helfrich, 1987. Effect of voltage on pores in membranes. *Phys. Rev. A* 36:5874-5876.
- [25] Bloomfield, V.A., D.M. Crothers and I. Tinoco, 1999. *Nucleic acids: structures, properties and functions* (University Science Books, Sausalito).
- [26] Vaughn, E.E., J.V. DeGiulio and D.A. Dean, 2006. Intracellular trafficking of plasmids for gene therapy: mechanisms of cytoplasmic movement and nuclear import. *Curr Gene Ther.* 6:671-681.
- [27] Lam, A.P. and D.A. Dean, 2010. Progress and prospects: nuclear import of non-viral vectors. *Gene Ther.* 12:439-447.

7. Figures

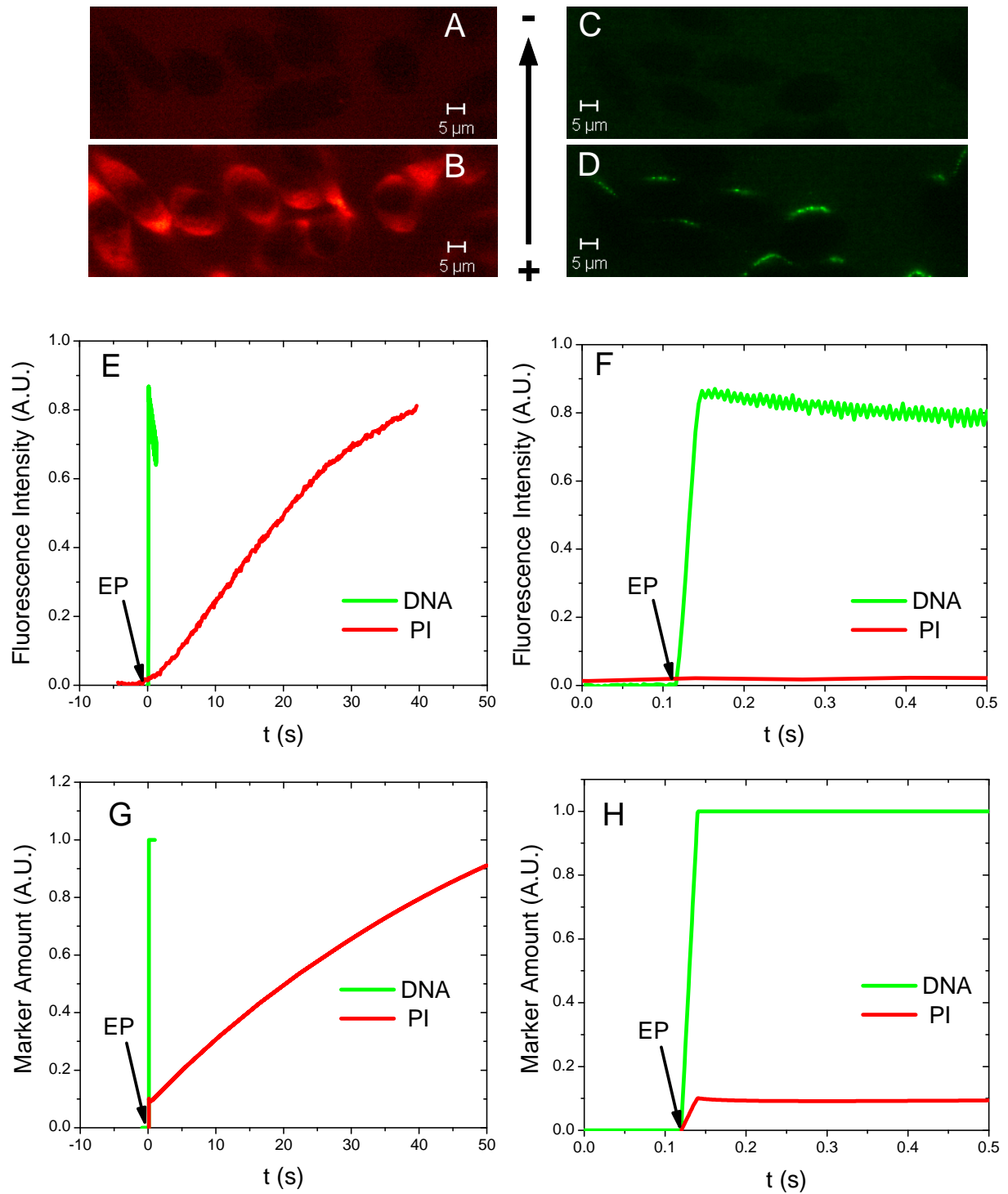


Figure 1: **Results and theoretical predictions of uptake of PI and DNA by electropulsed cells.** 1A and 1B: cells in the presence of PI and DNA before electropulsation, there is clearly no uptake of either marker. 1C: uptake of PI by cells after being electropulsed. 1D: interaction of DNA and cells after being electropulsed. 1E: long time behavior of PI (red) and DNA (green) uptake measured from the corresponding fluorescence. 1F: same data shown over a shorter time scale. 1G: long term uptake of PI and DNA as predicted by the electrodiffusion model. 1H: corresponding behavior over shorter time scale.

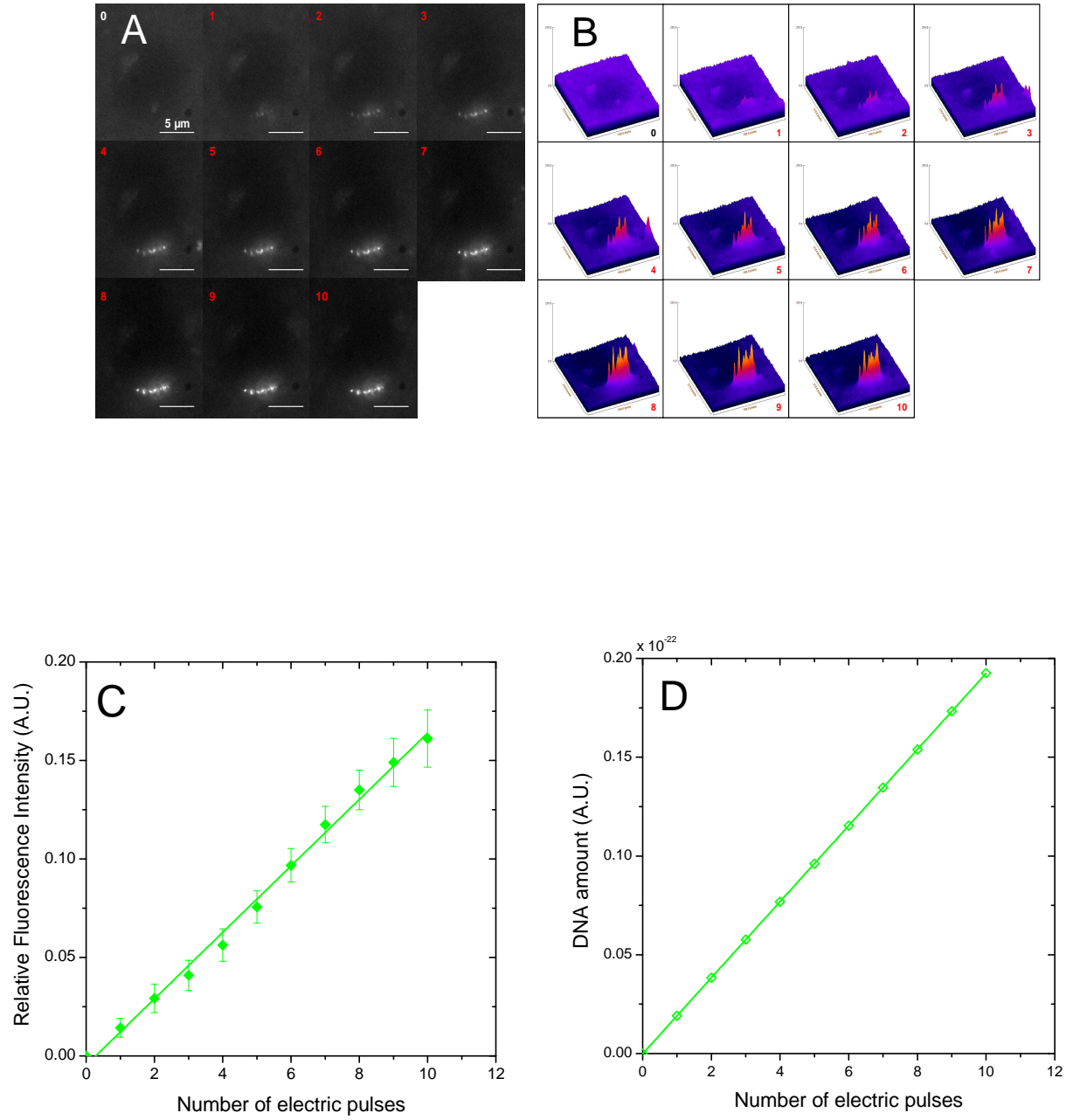


Figure 2: **Evolution of DNA fluorescence at interaction sites as a function of the number of electropulses.** 2A raw imaging data. 2B: quantified increase in DNA fluorescence based on a digital analysis of 2A. 2C: experimentally measured increase of total fluorescence due to DNA uptake as a function of the number of applied pulses. 2D: increase in DNA fluorescence as a function of the number of pulses as predicted by the electrodiffusion model.